

Multiscale Control for Nanoprecision Positioning Systems With Large Throughput

Huzefa Shakir, *Student Member, IEEE*, and Won-jong Kim, *Senior Member, IEEE*

Abstract—A problem of continuing interest in feedback control is handling conflicting time-domain performance specifications. Semiconductor manufacturing is one of the applications of particular interest in this context with the demanding feature sizes (on the order of a few tens of nanometers) to be produced on a wafer while still requiring high throughput (greater than 100 wafers per hour). In this brief, we propose a multiscale control design method based on a reduced-order model-following scheme for the dynamic systems with such conflicting time-domain performance requirements. This method uses a dynamic reference model to make the plant output track the model output as closely as possible without increasing the overall order of the control system. Optimal proportional–integral (PI) control is used, which is essentially a modification of the conventional optimal control. A detailed analytical proof is given to show that this control scheme effectively overcomes the limitations of the conventional optimal control techniques and provides consistent performances at nano- as well as macroscale positioning with fast rise and settling times. Benefits and limitations of the proposed control scheme are described and stability and performance analyses are discussed. A six-degree-of-freedom (6-DOF) extended-range magnetically levitated (maglev) nanopositioning stage, which is open-loop unstable, is used as a test bed to demonstrate the developed control strategy. Step responses under a variety of conditions are obtained to verify the effectiveness of the proposed method. This method exhibits significantly better and robust performances in terms of transient as well as steady-state behavior compared with conventional optimal-control schemes. Furthermore, it can be applied to a general class of higher-order linear time-invariant (LTI) systems with or without open-loop instability.

Index Terms—Multiscale control, nanopositioning, optimal proportional–integral (PI) control, reduced-order model following, semiconductor manufacturing.

I. INTRODUCTION

A PROBLEM of continuing interest in feedback control is handling the performance specifications of a controller to meet given time-domain characteristics, some or all of which may be conflicting in nature. In particular, the desired performance specifications may require 1) fast responses (in rise and settling times) with little or no overshoot and 2) large travel ranges with nanometer-level position resolution. Fast response is important in applications such as a manipulator's pick-and-place operations near a wall, filling a tank with fluid

in minimum time without spilling over, and temperature control in hazardous environment. Fine position resolution and high accuracy are required in positioning applications such as microstereolithography, nanopositioning, and scanning and imaging of nanoscale phenomena. In these applications, however, there is a notable tradeoff between the position accuracy and the process throughput, particularly in the applications requiring large travel ranges. High position accuracy can be achieved for large travel if the scan speed is kept very slow. However, in commercial applications like semiconductor manufacturing, high position resolution as well as throughput is important. We use the term *multiscale control* throughout this brief in order to emphasize the fact that such a control is capable of meeting such conflicting time-domain performance specifications and providing desired performances in both nano- and macroscale operations.

Despite the advancement in the control theory over the last few decades, this problem of dealing with conflicting time-domain performance specifications remains open. One reason is that there is no analytic relationship between the system parameters and the time-domain transient-response characteristics for systems of the order higher than two [1]. Even with the conventional optimal control techniques, the problem cannot be completely solved. The controllers tuned for load changes tend to produce large overshoots for reference tracking, whereas those tuned for reference tracking would result in sluggish recovery from load disturbances. We will further demonstrate this fact using an example of a maglev positioner in Section IV-A (see Fig. 2). A detailed description of the conventional optimal proportional–integral (PI) control and the difficulties associated with it is given in Section II.

Several methods were suggested in literature to achieve time-domain performance specifications using various control techniques. Phillips and Seborg [2] gave the conditions for nonovershooting feedback control systems for linear systems. Jayasuriya and Dharne [3] described the conditions for nonovershooting and nonundershooting responses based on the number of nonminimum-phase plant zeros. Moore and Bhattacharyya [1] proposed controller synthesis based on a zero-placement method to achieve nonovershooting step responses. Datta *et al.* [4] and Ho [5] designed fixed-order constant gain, PI and proportional–integral–derivative (PID) controllers, which met the specified time-domain characteristics. Some of them are based on several assumptions, like open-loop stability of the plant, a prespecified relationship between the zeros and poles of the plant, or a strictly proper single-input-single-output (SISO) plant [2], [3]. The developed control methods also have several limitations. Some of them require solving a partially finite convex programming problem while others involve searching for a solution over

Manuscript received October 24, 2006. Manuscript received in final form January 3, 2007. Recommended by Guest Editor E. Eleftheriou. This work was supported by the National Science Foundation under Grant CMS-0116642.

H. Shakir was with the Department of Mechanical Engineering, Texas A&M University, College Station, TX 77843-3123 USA. He is now with Halliburton Energy Services Inc., Houston, TX 77032 USA (e-mail: huzefa@tamu.edu).

W.-J. Kim is with the Department of Mechanical Engineering, Texas A&M University, College Station, TX 77843-3123 USA (e-mail: wjkim@tamu.edu).

Digital Object Identifier 10.1109/TCST.2007.902957

the entire set of the stability region, which may be unbounded [5]. Furthermore, the synthesized controllers may be of a very high order and thus affect the overall robust stability of the closed loop [6]. This motivates the need to develop multiscale control schemes that can satisfy the time-domain performance specifications in a unified way. It turns out that by relieving the constraint of overshoot from strictly nonovershooting to suboptimally overshooting, the problem under discussion may be much simplified. Suitable modifications of the existing optimal control techniques can provide significant improvements in time-domain performances. Besides, if full-state feedback is available, the excellent stability margin of optimal control is an added advantage.

In this brief, we present a multiscale control technique based on reduced-order model following that can be used to achieve these desired yet conflicting time-domain performance specifications. It uses a dynamic reference model without increasing the overall order of the system. The objective of this scheme is to make the plant's output track the model's output as closely as possible. Optimal PI control is used as a basis for the controller design. The reason for this choice is its popularity in most industrial applications. PI controllers are often effective and are easy to implement and maintain. Additionally, the results from optimal control methods are well-known to minimize the control effort and guarantee robust stability margins, particularly if full-state feedback is available. Furthermore, the inclusion of the integral term ensures the zero steady-state error for type-0 plants or the plants whose parameters are not perfectly known. We will elaborate this claim in Section IV with the example of a maglev positioner, which is type-0. Two other methods, namely controller-switching technique and integral reset scheme, are also briefly described. All these methods exhibit better performances compared with conventional control schemes.

A six-degree-of-freedom (6-DOF) maglev nanopositioner is used as a test bed to demonstrate the effectiveness of these control schemes. This maglev stage has demonstrated a positioning noise as small as 18 nm (peak-to-peak) over a control bandwidth of 110 Hz [7]. However, it has several inherent disadvantages and limitations: 1) a maglev system is open-loop unstable; 2) it tends to produce large overshoots due to absence of any contact or damping in the system; and 3) its actual plant model is highly nonlinear and a linearized model is not very accurate. All these challenges make the maglev positioner a good candidate to demonstrate the proposed control method.

This brief is organized as follows. Section II gives an overview of the conventional optimal PI control and its limitations. In Section III, we propose the multiscale control method using a reduced-order model-following scheme. The method is discussed analytically, addressing issues related to the effectiveness of the control method, stability, and input and output sensitivities. Section IV presents the experimental verification and validation of the proposed method using a 6-DOF maglev positioner as a test bed. Several step responses are given to demonstrate the benefits of this control scheme over traditional optimal control, the effect of initial mismatches in the plant states, and the effectiveness of this method to perform equally well at nano- as well as macroscale. Conclusions are presented in Section V.

II. CONVENTIONAL OPTIMAL CONTROL

In this section, we briefly discuss the conventional optimal PI controllers. It is usually desirable to include the integral action in optimal control systems in order to eliminate the offset due to unmeasured load disturbances or modeling errors. Consider an linear time-invariant (LTI) system

$$\begin{aligned}\dot{\mathbf{x}}_p &= A_p \mathbf{x}_p + B_p \mathbf{u}_p \\ \mathbf{y}_p &= C_p \mathbf{x}_p\end{aligned}\quad (1)$$

where \mathbf{x}_p is the state vector of dimension n , \mathbf{u}_p is the control vector of dimension r , \mathbf{y}_p is the output vector of dimension m , and A_p , B_p , and C_p are constant matrices of appropriate dimensions. This system is assumed to be controllable. It is also assumed that full-state feedback is available. Its unavailability would not affect the rest of the following analysis. However, robust stability could not be guaranteed in that case. For piecewise-constant, nonzero-reference points, an analogous PI control law can be obtained by redefining the state and output vectors. Let \mathbf{y}'_p be the p -dimensional subset of \mathbf{y}_p for which the integral action is desired. It is assumed that $p \leq r$ since there are only a total of r degrees of freedom [8]. Then the augmented system can be described as

$$\begin{aligned}\begin{bmatrix} \dot{\mathbf{e}}_{x_p} \\ \dot{\boldsymbol{\xi}}_p \end{bmatrix} &= \begin{bmatrix} A_p & 0 \\ C'_p & 0 \end{bmatrix} \begin{bmatrix} \mathbf{e}_{x_p} \\ \boldsymbol{\xi}_p \end{bmatrix} + \begin{bmatrix} B_p \\ 0 \end{bmatrix} \mathbf{e}_{u_p} \\ \begin{bmatrix} \mathbf{e}_{y_p} \\ \boldsymbol{\xi}_p \end{bmatrix} &= \begin{bmatrix} C_p & 0 \\ 0 & I \end{bmatrix} \begin{bmatrix} \mathbf{e}_{x_p} \\ \boldsymbol{\xi}_p \end{bmatrix} \\ \text{or } \dot{\tilde{\mathbf{x}}}_p &= \tilde{A}_p \tilde{\mathbf{x}}_p + \tilde{B}_p \mathbf{e}_{u_p} \\ \tilde{\mathbf{y}}_p &= \tilde{C}_p \tilde{\mathbf{x}}_p\end{aligned}\quad (2)$$

with the new set of variables $\mathbf{e}_{x_p} = \mathbf{x}_p - \mathbf{x}_R$, $\mathbf{e}_{y_p} = \mathbf{y}_p - \mathbf{y}_R$, $\mathbf{e}_{u_p} = \mathbf{u}_p - \mathbf{u}_R$, and $\mathbf{y}'_p = C'_p \mathbf{x}_p$, where C'_p is the appropriate partition of C_p , and the subscript R denotes the reference values of the corresponding variables. Furthermore, the set of integral state variables, $\boldsymbol{\xi}_p$ is defined as

$$\boldsymbol{\xi}_p(t) = \int_0^t (\mathbf{y}'_p(\tau) - \mathbf{y}'_R) d\tau. \quad (3)$$

Let \tilde{J} denote the performance index for the augmented system

$$\begin{aligned}\tilde{J} &= \frac{1}{2} \int_0^{\infty} (\mathbf{e}_{y_p}^T Q \mathbf{e}_{y_p} + \boldsymbol{\xi}_p^T Q_I \boldsymbol{\xi}_p + \mathbf{e}_{u_p}^T R \mathbf{e}_{u_p}) dt \\ &= \frac{1}{2} \int_0^{\infty} (\tilde{\mathbf{y}}_p^T \tilde{Q} \tilde{\mathbf{y}}_p + \mathbf{e}_{u_p}^T R \mathbf{e}_{u_p}) dt\end{aligned}\quad (4)$$

where $\tilde{Q} = \begin{bmatrix} Q & 0 \\ 0 & Q_I \end{bmatrix}$. If the augmented system is controllable, the optimal control law is given by

$$\mathbf{e}_{u_p} = -R^{-1} \tilde{B}^T \tilde{P} \tilde{\mathbf{x}}_p = -K \tilde{\mathbf{x}}_p \quad (5)$$

where \tilde{P} satisfies the algebraic Riccati equation. The control law in (5) can also be expressed as

$$\mathbf{u}_p = \mathbf{u}_R + K_C(\mathbf{x}_R - \mathbf{x}_p) + K_I \int_0^t (\mathbf{y}'_R - \mathbf{y}'_p) d\tau \quad (6)$$

where K_C and K_I are appropriate partitions of K in (5).

Equation (6) gives the optimal PI control law for the general nonzero reference-tracking problem. The control gain matrices K_C and K_I are determined by the choice of the weight matrices Q , Q_I , and R . These weight matrices are often treated as the tuning parameters for a given control application. Although the integral-control action is essential to eliminate the tracking error, the choice of the weight matrices in the quadratic performance index (4) usually involves a compromise between load-change and reference-tracking performances. In Section III, we propose a remedy for this problem based on modifications of the conventional optimal PI control.

III. MULTISCALE CONTROL

One viable choice to deal with the problem discussed in Section II is to design multiple controllers *a priori* to meet these conflicting objectives separately. The two controllers are then put into use sequentially. For practical reasons, it is preferred to ramp the transition from one set of controller gains to another in order to avoid any instability. Another promising solution is to limit the size of the integral term during the time period until a new reference point is reached. This strategy is equivalent to converting a tracking problem to a regulation problem after a certain period of time. This method makes full use of the integral control action in the beginning and hence, does not increase the rise time.

However, in many applications, it is desirable to use only one set of control parameters for reference tracking as well as load changes. On the other hand, it is also desirable to have small overshoot and fast response time without causing additional controller complexity or increasing the order of the plant model associated with the model-following approach. In the following subsections, we will focus on the development of a reduced-order model-following scheme and its analyses in terms of stability, transient and steady-state behavior, and closed-loop criteria such as sensitivity function, bandwidth, and control effort.

A. Reduced-Order Model-Following Scheme

A reduced-order model-following approach may be used to solve the multiscale control problem. Conventional model following schemes try to make the output of the plant \mathbf{y} follow the output of a reference model \mathbf{y}_m as closely as possible. The reference model is a dynamic model which has \mathbf{y}_R as its input vector. A major disadvantage of the model-following scheme is that the original system's state vector is appended with the model's states, and hence the overall plant order increases. This requires a higher-order Riccati equation to be solved and an additional gain matrix to be stored.

A modified version of the model-following scheme is used here that does not require any additional states. Consider a reference model of the form

$$\begin{aligned} \dot{\mathbf{x}}_m &= A_m \mathbf{x}_m + B_m \mathbf{u}_m \\ \mathbf{y}_m &= C_m \mathbf{x}_m. \end{aligned} \quad (7)$$

The A_m , B_m , and C_m matrices in this reference model are assumed to be the same as those of the plant in (1). An approach to ensure that the reference model has a suitable reference-tracking response with little or no overshoot is to specify \mathbf{u}_m as

$$\mathbf{u}_m = \mathbf{u}_R + K_C(\mathbf{x}_R - \mathbf{x}_m) \quad (8)$$

where K_C is the control gain matrix specified in (6). Using an analogous derivation as outlined in Section II, we get

$$\begin{aligned} \dot{\tilde{\mathbf{x}}}_m &= \tilde{A}_m \tilde{\mathbf{x}}_m + \tilde{B}_m \mathbf{e}_m \\ \tilde{\mathbf{y}}_m &= \tilde{C}_m \tilde{\mathbf{x}}_m. \end{aligned} \quad (9)$$

Define $\delta \mathbf{x} = \tilde{\mathbf{x}}_p - \tilde{\mathbf{x}}_m$, $\delta \mathbf{y} = \tilde{\mathbf{y}}_p - \tilde{\mathbf{y}}_m$, and $\delta \mathbf{u} = \mathbf{u}_p - \mathbf{u}_m$. Then, the error dynamics is

$$\begin{aligned} \delta \dot{\mathbf{x}} &= \tilde{A}_p \delta \mathbf{x} + \tilde{B}_p \delta \mathbf{u} \\ \delta \mathbf{y} &= \tilde{C}_p \delta \mathbf{x}. \end{aligned} \quad (10)$$

The optimal PI control law for this plant is given by

$$\mathbf{u}_p = \mathbf{u}_m + K_C(\mathbf{x}_m - \mathbf{x}_p) + K_I \int_0^t (\mathbf{y}'_m - \mathbf{y}'_p) d\tau. \quad (11)$$

Using (8) and (11), we get

$$\mathbf{u}_p = \mathbf{u}_R + K_C(\mathbf{x}_R - \mathbf{x}_p) + K_I \int_0^t (\mathbf{y}'_m - \mathbf{y}'_p) d\tau. \quad (12)$$

This control law has essentially the same structure as that of the conventional optimal PI control given by (6) with \mathbf{y}'_R replaced by \mathbf{y}'_m in the integral term.

It may be proven that the reduced-order model-following scheme reduces the problem of overshoot subject to some conditions. Consider the plant and model dynamics defined by (1) and (7), respectively. The reference input dynamics is given by

$$\dot{\mathbf{x}}_R = \mathbf{0} = A_p \mathbf{x}_R + B_p \mathbf{u}_R. \quad (13)$$

Using the new set of variables defined in (10) and substituting the control law from reduced-order model following scheme (11) in (1), we get

$$\dot{\mathbf{x}}_p = (A_p - B_p K_C)(\mathbf{x}_p - \mathbf{x}_R) + B_p K_I C'_p \int_0^t (\mathbf{x}_m(\tau) - \mathbf{x}_p(\tau)) d\tau. \quad (14)$$

Similarly, using the new set of variables defined in (9) and using control law (8), we get

$$\dot{\mathbf{x}}_m = (A_p - B_p K_C)(\mathbf{x}_m - \mathbf{x}_R). \quad (15)$$

Subtracting (15) from (14), we get

$$\dot{\mathbf{x}}_p - \dot{\mathbf{x}}_m = (A_p - B_p K_C)(\mathbf{x}_p - \mathbf{x}_m) - B_p K_I C'_p \times \int_0^t (\mathbf{x}_p(\tau) - \mathbf{x}_m(\tau)) d\tau. \quad (16)$$

Differentiating (16) with respect to t gives

$$\ddot{\mathbf{x}}_p - \ddot{\mathbf{x}}_m = (A_p - B_p K_C)(\dot{\mathbf{x}}_p - \dot{\mathbf{x}}_m) - B_p K_I C'_p (\mathbf{x}_p - \mathbf{x}_m) \quad (17)$$

with initial condition $\mathbf{x}_p(0) - \mathbf{x}_m(0) = \mathbf{0}$. Therefore, from (16), we have $\dot{\mathbf{x}}_p(0) - \dot{\mathbf{x}}_m(0) = \mathbf{0}$. The solution of (17) with these initial conditions is given by

$$\mathbf{x}_m(t) = \mathbf{x}_p(t). \quad (18)$$

Equation (18) shows that the model states follow the plant states. Furthermore, the integral term in (16) is eliminated, provided 1) the initial states of the model are equal to those of the plant and 2) the plant and model system matrices are identical. In the presence of modeling errors, the integral windup will be small as long as the model output \mathbf{y}_m is close to the plant output \mathbf{y}_p . Thus, the problem of excessive overshoot due to integral action is reduced without increasing the closed-loop plant order, requiring different controller gains and subsequent controller switching, or requiring the perfect knowledge of the plant transfer function (TF) or initial plant states. We will further discuss the effect of mismatch between the initial plant and model states in Section IV.

B. Stability and Performance Analyses

Since we are using modified optimal linear-quadratic (LQ) control methodologies to design the controllers and since full state feedback is available, we have the advantage of the guaranteed stability margins, i.e., the gain margin between 6 dB and ∞ , and the phase margin greater than 60° [9]. This may be verified by doing a Nyquist stability analysis at any loop-breaking point in the closed loop.

Robustness analysis may be done similarly for process and measurement noises. Consider the combined closed-loop system given by

$$\begin{bmatrix} \dot{\tilde{\mathbf{x}}}_p \\ \dot{\tilde{\mathbf{x}}}_m \\ \tilde{\mathbf{y}}_p \\ \tilde{\mathbf{y}}_m \end{bmatrix} = \begin{bmatrix} \tilde{A}_p & 0 \\ 0 & \tilde{A}_p \end{bmatrix} \begin{bmatrix} \tilde{\mathbf{x}}_p \\ \tilde{\mathbf{x}}_m \end{bmatrix} + \begin{bmatrix} \tilde{B}_p & 0 \\ 0 & \tilde{B}_p \end{bmatrix} \begin{bmatrix} \mathbf{e}_{u_p} + \mathbf{d} \\ \mathbf{e}_{u_m} \end{bmatrix} \\ \begin{bmatrix} \tilde{\mathbf{y}}_p \\ \tilde{\mathbf{y}}_m \end{bmatrix} = \begin{bmatrix} \tilde{C}_p & 0 \\ 0 & \tilde{C}_p \end{bmatrix} \begin{bmatrix} \tilde{\mathbf{x}}_p \\ \tilde{\mathbf{x}}_m \end{bmatrix} + \begin{bmatrix} \mathbf{n} \\ \mathbf{0} \end{bmatrix} \quad (19)$$

where \mathbf{d} and \mathbf{n} are process and measurement noises as indicated in Fig. 1. The input sensitivity TF T_d for this system from the input disturbance \mathbf{d} to the plant outputs $\tilde{\mathbf{y}}_p$ is given by

$$\|T_d\| = \left\| (sI - \tilde{A}_p + \tilde{B}_p K)^{-1} \tilde{B}_p \right\|. \quad (20)$$

Likewise, the output sensitivity TF T_n from measurement noise \mathbf{n} to the plant outputs is given by

$$\|T_n\| = \left\| (sI - \tilde{A}_p + \tilde{B}_p K)^{-1} \tilde{B}_p K \right\|. \quad (21)$$

Stability of the closed-loop system at the loop-breaking point "A" (see Fig. 1) and an analysis of the performance of the proposed scheme in the presence of both process and measurement

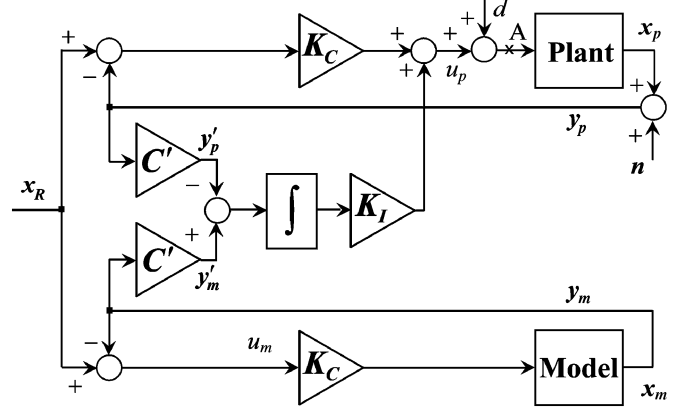


Fig. 1. Block diagram representing the multiscale control scheme.

noises will be demonstrated with the maglev nanopositioner example in Section IV. We conclude this section by making a remark that we carried out the entire design on a generic state-space model of an n th-order plant with r inputs and m outputs. Thus, the method discussed in this section is valid for any LTI plant with higher order as long as the assumptions and conditions noted in Sections II and III are valid.

IV. MAGLEV NANOPositionER EXAMPLE

We used a 6-DOF maglev nanopositioner to test the proposed control scheme and demonstrate its performance. This maglev stage comprises a moving element and six stationary electromagnetic coils for actuation. The most notable feature of this positioner is that the moving platen is a simple single-part structure that is capable of accurate positioning with a large travel range and high speed in all 6-DOFs [7]. It has an extended planar travel range of 5×5 mm with a positioning noise of 18 nm (peak-to-peak) over a 110-Hz control bandwidth. The six-axis motions are generated by appropriate combinations of six independent force components from the actuators. Horizontal position and velocity of the platen is measured by three single-axis laser interferometers at subnanometer resolution. For vertical motion sensing, we have three capacitance gauges mounted on the base plate right below the platen. Real-time digital control is implemented and performed on a digital signal processor (DSP) at a sampling frequency of 5 kHz. System identification is necessary in order to get an accurate plant model and subsequently to design reliable control strategies. It is not only crucial but also challenging because of the inherently unstable nature of magnetic levitation. Thus, the Box-Jenkins (BJ) method with a closed-loop framework and a known controller structure is used to obtain the closed-loop TF [10]. The identified continuous-time state-space plant model for the x -axis motion is given by

$$\begin{aligned} \dot{\mathbf{x}}_p &= \begin{bmatrix} -5.69 & 1 \\ 5477.53 & 0 \end{bmatrix} \mathbf{x}_p + \begin{bmatrix} 0 \\ 3.19 \end{bmatrix} u_p \\ \mathbf{y}_p &= \begin{bmatrix} 1 & 0 \\ 0 & 1 \end{bmatrix} \mathbf{x}_p \end{aligned} \quad (22)$$

where the state vector \mathbf{x}_p consists of the position and velocity of the maglev positioner, the control input u_p is the force required along the x -axis and the output vector \mathbf{y}_p consists of the

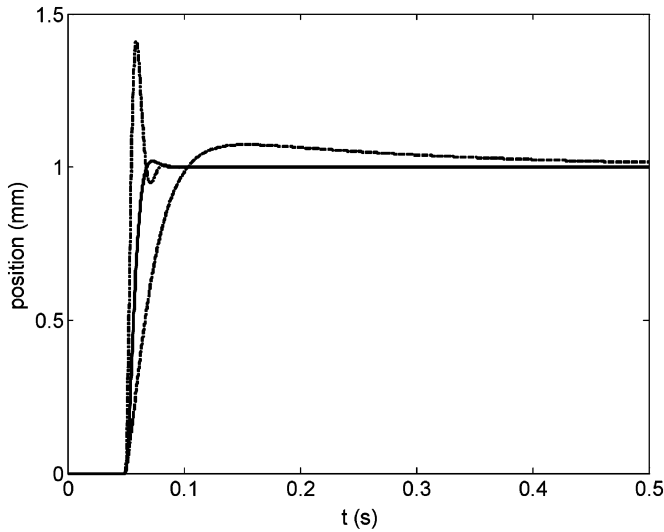


Fig. 2. 1-mm step responses in x with the multiscale control scheme with $Q_I = 10^{12}$ (solid line), and conventional LQ controllers with $Q_I = 10^8$ (dashed line) and $Q_I = 10^{14}$ (dashed-dotted line).

sensed position and velocity data from the laser interferometers. Plant models in other five axes may be identified and used for controller design in a similar manner and are omitted in this brief for brevity. Note that there is one right-half plane pole in the identified plant model, which correctly reflects the maglev system's open-loop instability due to the negative stiffness of the magnetic origin.

An LQ optimal controller was designed for this system following the method discussed in Section II. Since we are primarily interested in positioning, we use the integral action for position control only. The weight matrices were chosen to be $\tilde{Q} = \text{diag}([2 \times 10^6, 1 \times 10^3, 1 \times 10^{12}])$ and $R = 1$ after a few iterations, starting with using acceptable values of \mathbf{x}_p and u_p based on the sensing range of the laser interferometers and actuator saturation limits, such that $\tilde{Q}_{ii} = 1/\max|x_{ii}|^2$ and $R = 1/\max|u_{ii}|^2$.

A. Transient and Steady-State Performance

A block diagram showing the implementation of the proposed control scheme on the plant model (22) is shown in Fig. 1. Step responses to a 1-mm command using the conventional optimal control as well as the proposed multiscale control are shown in Fig. 2. They support our claim made in Section I that a single controller cannot be used to achieve good load-change as well as reference-tracking performance objectives. The reduced-order model-following scheme, on the other hand is capable of meeting both the objectives with a single set of controller gains, and without requiring any abrupt changes in the gain values. Fig. 3 shows the 1-mm and 100-nm step responses for positive and negative steps, normalized to unity for comparison. The plot demonstrates that the multiscale control scheme gives almost identical performances at nano- as well as macroscale, except for the noise level, thus justifying the term *multiscale* as we defined in the Section I. It also shows that the controller design results in repeatable performance and

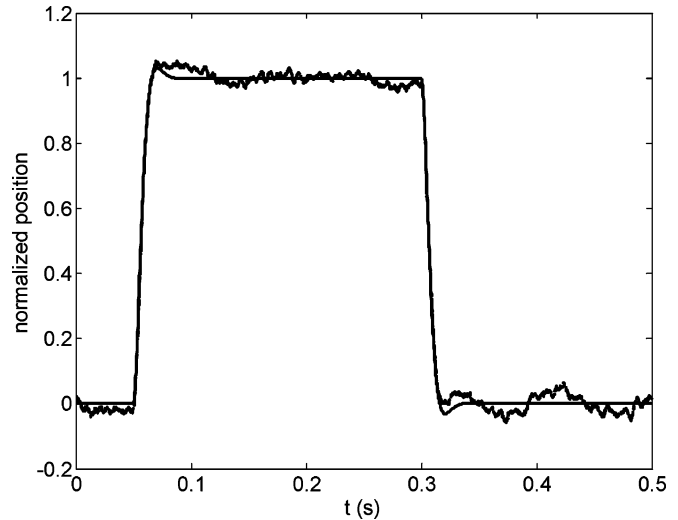


Fig. 3. 1-mm (solid line) and 100-nm (dashed line) step responses, normalized to 1 for comparison, with the proposed multiscale control scheme.

the results presented herein are not based on a single set of experiments.

B. Performance With Initial-State Mismatch

In Section III, we demonstrated that the integral term of the controller is eliminated provided the initial states match perfectly. Furthermore, in the presence of modeling errors, the integral windup will be small as long as the model output \mathbf{y}_m is close to the plant output \mathbf{y}_p . Here, we demonstrate that even in the presence of initial-state mismatches as much as $\pm 20\%$, the model states converge to the plant states in about the same time as without any mismatch. This percentage is chosen only to demonstrate the effect of mismatch; the plant states track the desired reference inputs no matter how large the initial mismatch. Fig. 4 demonstrates this situation where the initial state vector of the model is not identical to that of the actual plant. The model states are shown with solid lines while the actual plant states are shown with dashed (+20% mismatch) and dashed-dotted lines (−20% mismatch). With imperfect knowledge of initial plant states, the dynamic performance is moderately affected in terms of overshoot. However, there is no significant change in the rise and settling times and the steady-state errors. Furthermore, the model states converge to plant states in almost the same time. This implies that for any reference-tracking problem, if the initial plant states are not known perfectly, a dummy step can be given to allow the model states to become identical to those of plant. Any subsequent meaningful tracking can then be done without any error.

C. Stability

Although it is apparent from the step responses shown in Figs. 2–4 that the multiscale control scheme results in stable control loops even in the presence of model uncertainties and initial-state mismatches, a formal stability analysis is still necessary to find how much uncertainty can be tolerated in the closed loop. Fig. 5 shows the Nyquist plot for the reduced-order model-following scheme at the loop-breaking point “A.” Since we have an unstable pole in the plant TF and the Nyquist plot

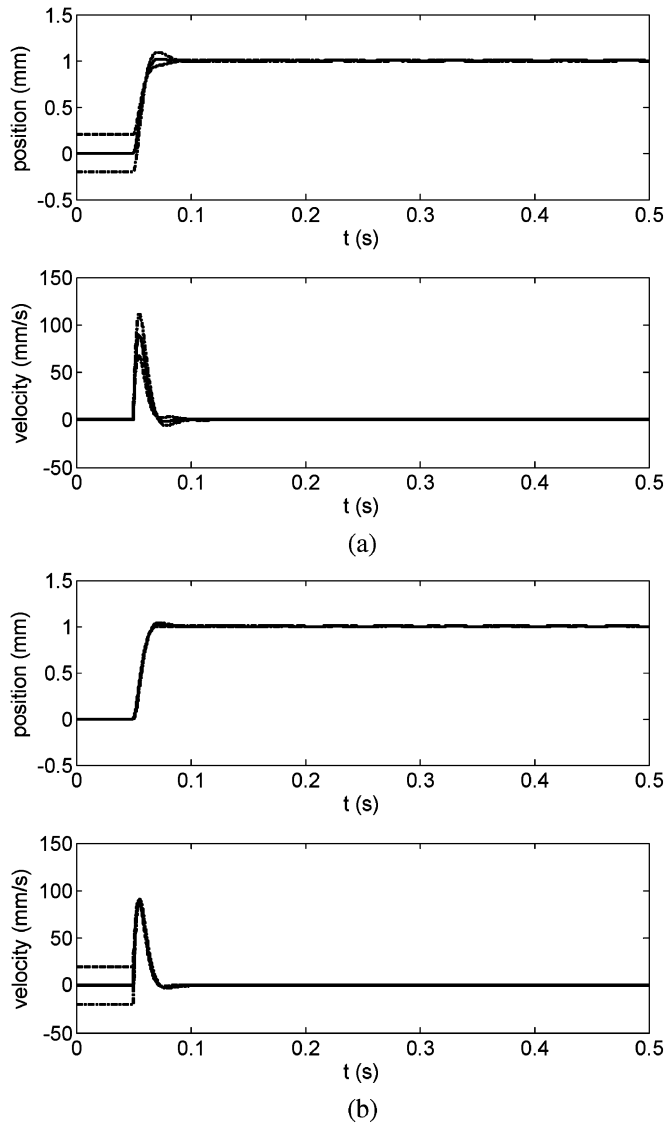


Fig. 4. Model states (solid line) and responses of the plant with multiscale control scheme in the presence of the mismatch between the plant and model initial states with a difference of +20% (dashed line) and -20% (dashed-dotted line) in (a) position and (b) velocity.

encircles the -1 point in the counterclockwise direction once, we have a stable closed loop from the Nyquist criteria. Furthermore, in this case, the closed-loop has a gain margin of at least 11.2 dB and a phase margin of at least 63° .

D. Performance in the Presence of Noises

Another analysis of particular interest is the robustness of the designed controller to process and measurement noises. Fig. 6 shows the input and output sensitivity TFs for the maglev positioner using (20) and (21). It may be concluded from Fig. 6 that the output of the plant is not affected significantly by the input disturbances. The process noise at the input end to the plant is physical in nature and is expected to be of low frequency. For the entire frequency range, the maximum amplification of these disturbances is around -80 dB at around 20 Hz. The measurement noises, on the other hand, have high-frequency contents. For the frequencies greater than 1 kHz, the amplification of the

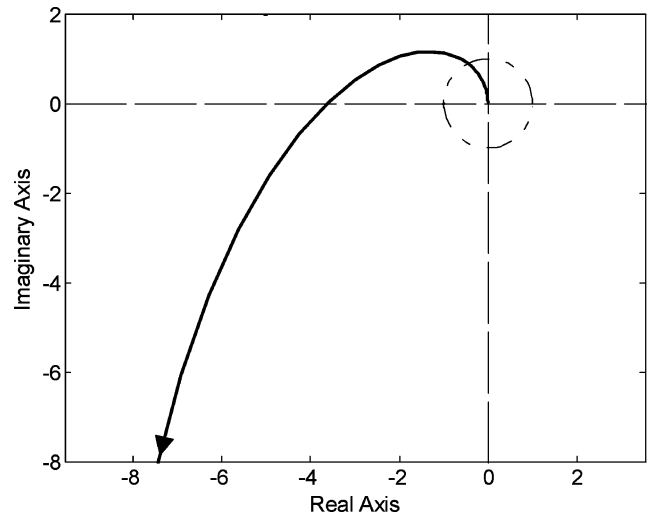


Fig. 5. Nyquist plot showing the stability margins of the multiscale control scheme at control-input loop-breaking point to the plant "A" in Fig. 1.

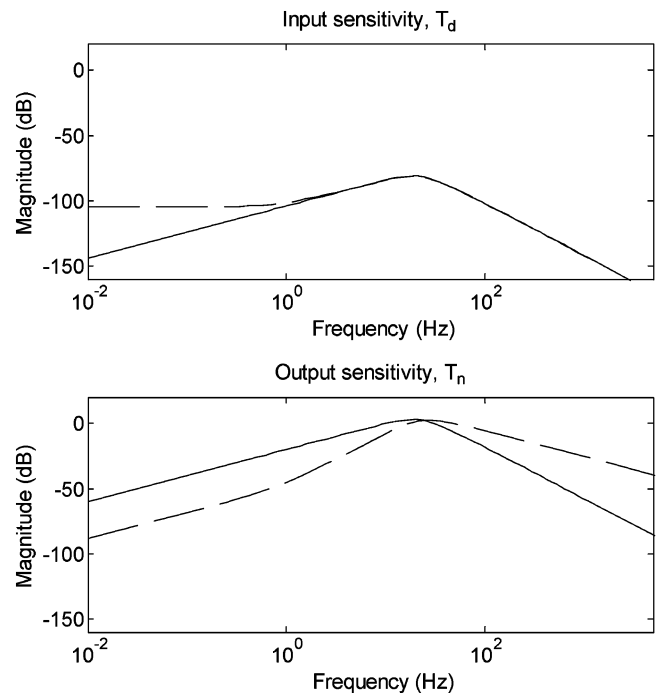


Fig. 6. Input sensitivity TFs between the control input disturbance d and the states position (solid line) and velocity (dashed line), and output sensitivity TFs between the measurement noises n and the respective states position (solid line) and velocity (dashed line).

position measurement is less than -60 dB, while that of velocity measurement is less than -25 dB. Thus, the multiscale control scheme offers almost the same level of performances even in the presence of process as well as measurement noises.

V. CONCLUSION

The main focus of this brief was to present a multiscale control technique that can be used to meet conflicting time-domain performance specifications at nano- as well as macroscale. In particular, emphasis was given to the requirement of achieving little or no overshoot with a zero steady-state error and fast dynamic response in terms of rise and settling times. Semicon-

ductor manufacturing is such an application wherein these performance objectives translate into achieving nanoscale feature sizes at high throughput.

The effectiveness, stability, and performance analyses of the proposed method were performed in detail. Emphasis was given on the fact that the proposed method does not increase the overall order of the closed-loop system unlike the traditional model-following schemes. A maglev nanopositioner was used as a test bed to demonstrate the working of this method on a practical system with problems like open-loop instability, unknown plant TF, imperfectly known initial plant states, and presence of process and measurement noises. The multiscale control scheme was found to provide significantly improved responses compared with the conventional optimal PI control.

In the experimental verification with the maglev nanopositioner, the designed controller gave almost identical performance for step sizes of 1 mm and 100 nm. The gain margin was found to be greater than 11.2 dB along with a phase margin of at least 63° . Furthermore, an initial mismatch between the plant and model states can also be sustained without losing stability or affecting the performance of the closed-loop significantly. In the presence of process and measurement noises for position, the attenuation is about -80 and -60 dB, respectively, in the frequency ranges of interest. The results presented herein were consistent and repeatable. Although only a linear system with a known plant model was considered, the proposed multiscale

control method works well with a general class of higher-order LTI systems with or without open-loop instability.

REFERENCES

- [1] K. L. Moore and S. P. Bhattacharyya, "A technique for choosing locations for minimal overshoot," *IEEE Trans. Autom. Control*, vol. 35, no. 5, pp. 577–580, May 1990.
- [2] S. F. Phillips and D. E. Seborg, "Conditions that guarantee no overshoot for linear systems," *Int. J. Control*, vol. 47, no. 4, pp. 1043–1059, 1988.
- [3] S. Jayasuriya and A. G. Dharne, "Necessary and sufficient conditions for non-overshooting step responses for LTI systems," in *Proc. Amer. Control Conf.*, 2002, pp. 505–510.
- [4] A. Datta, M.-T. Ho, and S. P. Bhattacharyya, "Structure and synthesis of PID controllers," in *Advances in Industrial Control*. New York: Springer, 2000, ch. 5.
- [5] M.-T. Ho, "Synthesis of \mathcal{H}_∞ PID controllers: A parametric approach," *Automatica*, vol. 39, no. 6, pp. 1069–1075, Jun. 2003.
- [6] L. H. Keel and S. P. Bhattacharyya, "Robust, fragile or optimal?," in *Proc. Amer. Control Conf.*, 1997, pp. 1307–1313.
- [7] W.-J. Kim and S. Verma, "Multi-axis maglev positioner with high resolution over large travel range," presented at the ASME Int. Mechan. Eng. Congr. Exp., 2005, Paper 80050.
- [8] R. B. Newell and D. G. Fisher, "Experimental evaluation of optimal multivariable regulatory controllers with model-following capabilities," *Automatica*, vol. 8, no. 3, pp. 247–262, May 1972.
- [9] S. Stogestad and I. Postlewaite, *Multivariable Feedback Control*. New York: Wiley, 2003.
- [10] R. Pintelon, Y. Rolain, and J. Schoukens, "Box-Jenkins identification revisited—Part II: Applications," *Automatica*, vol. 42, no. 1, pp. 77–84, Jan. 2006.